Progress In Electromagnetics Research C, Vol. 89, 161–169, 2019

A Compact Dual Band-Notched MIMO Diversity Antenna for UWB Wireless Applications

Yi Zhao*, Fu-Shun Zhang, Li-Xin Cao, and Deng-Hui Li

Abstract—In this paper, a compact ultra-wideband (UWB) multiple-input multiple-output (MIMO) spatial diversity antenna with dual band-notches designed on an FR4 substrate is proposed and experimentally investigated. The antenna consists of two radiating elements fed by two tapered microstrip lines. Two inverted L-shaped slits are used to introduce notches at WLAN (5.15–5.85 GHz) and IEEE INSAT/Super-Extended C-band (6.7–7.1 GHz). An isolation of more than 15 dB is achieved through the whole working band (2.9–10.8 GHz) by introducing a T-shaped decoupling structure on the ground plane. Furthermore, the envelope correlation coefficient (ECC), diversity gain (DG), multiplexing efficiency, TARC, peak gain and radiation patterns of the MIMO antenna are also discussed. The simulated and measured results show that the proposed UWB MIMO antenna is a good candidate for UWB diversity applications.

1. INTRODUCTION

Ultra-wideband (UWB) technologies, due to their advantages, such as low cost and high data rate, play an important role in modern wireless communications [1]. Nevertheless, multipath fading and channel fading will cause instability of UWB technology. To solve this problem, multiple-input-multiple-output (MIMO) technology has been proposed. By utilizing multiple directional beams to obtain independent signals, which use different radiation patterns to improve multipath fading problem and co-channel interference [2], MIMO is a key technology for UWB wireless communication systems.

In recent years, terminal devices tend to be miniaturized, and therefore serious mutual coupling will occur between antenna elements and other electronic components. Multifarious methods have been researched to decouple the radiating elements in UWB MIMO systems. In [3], in order to reduce the mutual coupling at lower frequency, two bent slots are etched into the ground plane. The antenna elements are placed perpendicularly in [4] and [5] to reduce mutual coupling in low frequency. Different parasitic structures were investigated to improve isolation in [6–9]. A compact printed UWB MIMO antenna with high isolation is presented in [10], which is obtained by adding slots and separating main radiation directions of two antenna elements, but the impedance bandwidth is not as wide as UWB requirements.

Another problem of MIMO antennas is the electromagnetic interference in the UWB, which was proclaimed permission from 3.1 GHz to 10.6 GHz for UWB communications in 2002. To deal with this problem, researchers have developed a great number of antennas. In [11], a half-wavelength resonant stub is embedded in the stepped-shaped slot to obtain a notched band, and the length of the stub is determined by the center frequency of the band. Two kinds of compact MIMO antenna with high isolation are presented for UWB applications in [12] and [13], where the notched band of 5.5 GHz is realized by etching a pair of L-shaped slits and an SRR. By etching an open slot and an SRR in the

Received 19 November 2018, Accepted 4 December 2018, Scheduled 3 January 2019
* Corresponding author: Yi Zhao (1367425852@qq.com).
The authors are with the National Key Laboratory of Antennas and Microwave Technology, Xidian University, Xi'an 710071, P. R. China.

Table 1. Comparison between the proposed antenna and the designs reported previously.

Reference	Size (mm^2)	Impedance bandwidth (GHz)	Notched band (GHz)	Isolation (dB)	ECC	Peak gain (dB)
[4]	32×32	3.10–10.60	-	-15	< 0.04	1.8–3.5
[6]	50×42	2.50–13.30	-	-15	< 0.2	-0.1–5.9
[8]	40×40	3.10–10.60	-	-15	-	-
[9]	42×40	3.10–7.20	-	-15	< 0.1	-
[11]	44×44	2.95–10.60	5.10–5.95	-15	< 0.04	1.5–4
[12]	38.5×38.5	3.08–11.80	5.03–5.97	-15.5	< 0.02	1–3.6
[13]	30×30	3.50–10.60	5.1–5.8 & 7.9–8.4	-15	< 0.05	0.5–5.2
[14]	48×48	2.50–12.00	5.1–6	-15	-	-
[17]	50×30	2.50–14.50	-	-20	< 0.04	0.2–4.2
proposed	26×28	2.90–10.80	5.05–5.86 & 6.68–7.43	-15	< 0.08	1.6–4

ground plane, a UWB MIMO antenna with two band notches was proposed in [14]. The decoupling structure is a Y-shaped defected ground structure. Many UWB MIMO antennas are listed in Table 1, in which all of them have relatively large size.

In this paper, a compact UWB MIMO spatial diversity antenna with dual band-notches is presented. The antenna is designed on an FR4 substrate with a compact size. The half-rectangle radiating elements fed by tapered microstrip feeding lines are designed to achieve UWB characteristics and spatial diversity. The defective ground with a T-shaped stub is used to improve impedance matching and ensure high isolations. Two inverted L-shaped slits are used to introduce notches at WLAN (5.15–5.85 GHz) and IEEE INSAT/Super-Extended C-band (6.7–7.1 GHz). The measurements denote that the proposed antenna is suitable for MIMO system.

2. ANTENNA GEOMETRY AND DESIGN

2.1. Antenna Configuration

Figure 1(a) describes the geometry of the proposed antenna. It is fabricated on a low-cost FR4 substrate with a relative dielectric constant of 4.4 and loss tangent of 0.02. The total size is $26 \times 28 \times 0.8\,mm^3$ or $0.27\lambda_0 \times 0.29\lambda_0 \times 0.01\lambda_0$, where λ_0 is the free-space wavelength at 3.1 GHz. It consists of two half-rectangle radiating elements, both fed by tapered microstrip feeding lines, which improve input impedance matching. Each radiator has two inverted L-shaped slits, each of which introduces a band notch. To ensure high isolation through the operating frequency, a T-shaped stub is introduced on the ground. The optimized dimensions are derived using ANSYS HFSS 15.0, shown in Figure 1(a): $W = 28\,mm$, $L = 26\,mm$, $W1 = 2\,mm$, $L1 = 10\,mm$, $W2 = 6\,mm$, $L2 = 8.95\,mm$, $W3 = 2.8\,mm$, $L3 = 3.5\,mm$, $W4 = 6\,mm$, $L4 = 4.5\,mm$, $W5 = 6\,mm$, $L5 = 15\,mm$, $W6 = 1.9\,mm$, $L6 = 6\,mm$, $L7 = 12\,mm$, $R = 2\,mm$. A picture of the fabricated antenna is shown in Figure 1(b). The performances of the antenna mentioned above are studied in detail as follows.

To better understand the design procedure of the radiating element, three antenna structures are modeled and simulated by ANSYS HFSS software, as shown in Figure 2. First, a half-rectangle radiating element fed by a tapered microstrip line (Antenna A) is designed to achieve UWB characteristics. After realizing UWB performance, the antenna is modified to introduce the WLAN (5.15–5.85 GHz) band notch as shown in Figure 2 with an inverted L-shaped slit (Antenna B). Finally, on the base of Antenna B, another slit is etched in the radiating element (Antenna C) to introduce IEEE INSAT/Super-Extended C-band (6.7–7.1 GHz) as shown in Figure 2. The effect of the slits will be discussed in detail in the next section. And the simulated $|S_{11}|$ for the three configurations is depicted in Figure 3.

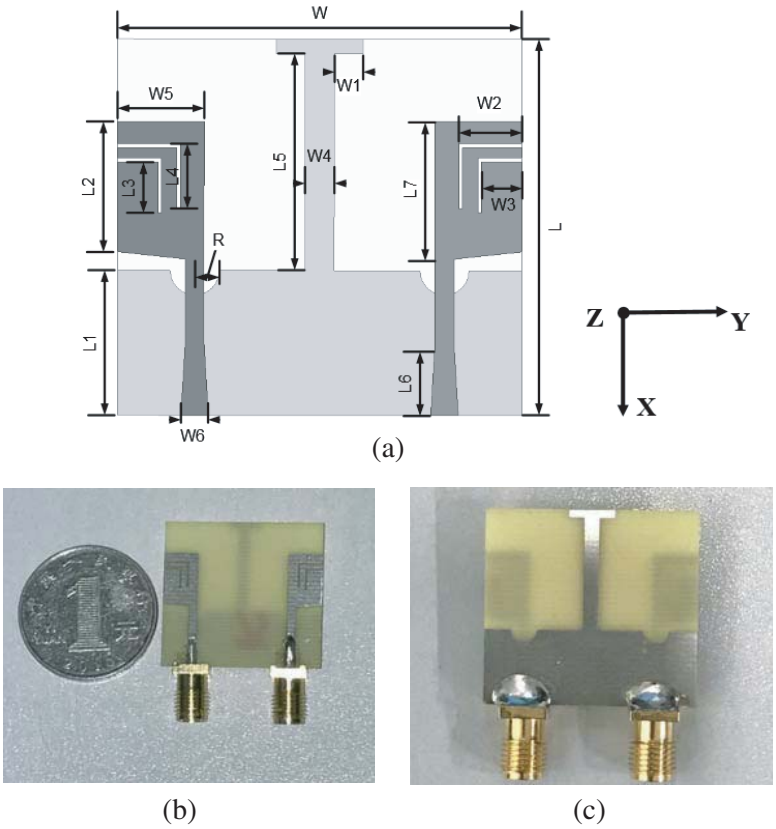

Figure 1. Proposed antenna geometry. (a) Structure of the proposed antenna. (b) Front view of the fabricated antenna. (c) Back view of the fabricated antenna.

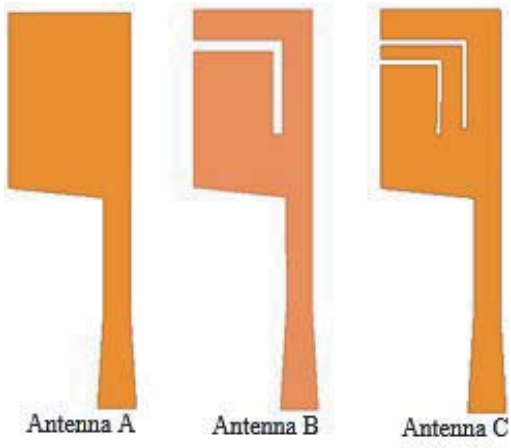

Figure 2. Configurations of the prototypes of Antenna A, B and C.

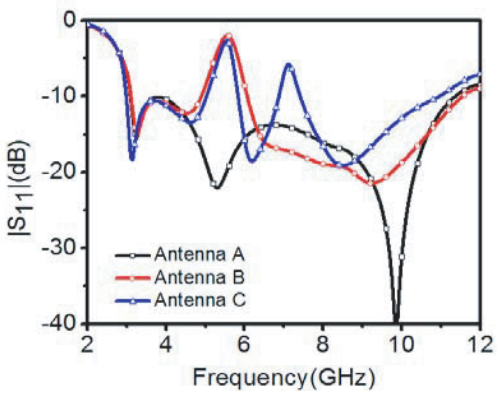

Figure 3. Simulated $|S_{11}|$ of Antenna A, B and C.

2.2. Effect of the Slits

The dual band-notched characteristics in the proposed antenna are introduced by two inverted L-shaped slits etched in each radiator. These L-shaped slits introduce impedance mismatching between the feeding line and radiating element as a $\lambda/4$ resonator, so that band-notched characteristics are achieved. The

slit length is about $\lambda/4$ at the center of the rejected band and can be calculated by [15]

$$L = \frac{c}{4f_{center} \cdot \sqrt{\varepsilon_{eff}}} \tag{1}$$

$$\varepsilon_{eff} \approx \frac{\varepsilon_r + 1}{2} \tag{2}$$

where ε_{eff} is the effective dielectric constant, and c is the speed of light.

The WLAN band is rejected by the upper etched slit, and the IEEE INSAT/Super-Extended C-band is rejected by the shorter etched slit. According to Eq. (1), the length of the upper slit is 8.3 mm, and the lower slit is 6.6 mm. In order to understand the effect of the etched slits in depth, Figure 4 plots the current distributions of the proposed antenna. From Figure 4, it is clear that the surface current is concentrated on the upper slit at 5.5 GHz and on the lower slit at 6.9 GHz. Besides that, the currents on the two sides of the slit are in opposite directions for both frequencies. As a result, radiation from both sides will counteract in the far fields. Therefore, little radiation occurs, and return loss is deteriorated. These current distributions indicate that the proposed antenna can achieve band rejection at the WLAN band and IEEE INSAT/Super-Extended C-band.

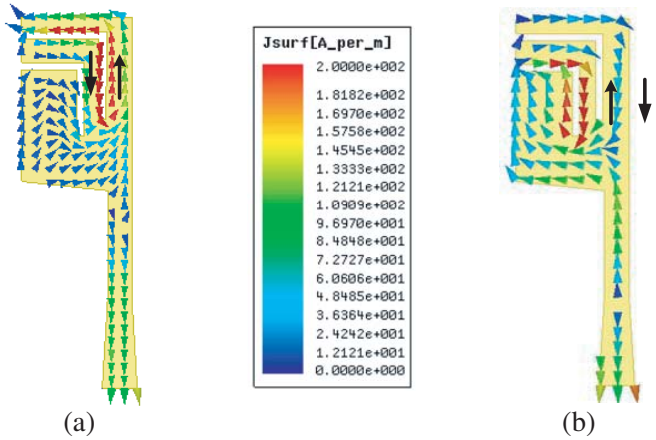

Figure 4. Simulated surface current distributions at different frequencies. (a) 5.5 GHz. (b) 6.9 GHz.

2.3. Effect of Ground

The ground plane has a significant impact on the performance of the presented antenna. The semi-circular slots on the ground are used to widen the impedance bandwidth. The rectangular stub on the ground is not only used for improving impedance matching, but also used for increasing isolation in the low operating frequency. Figure 5 shows the ground structure design steps of the UWB MIMO

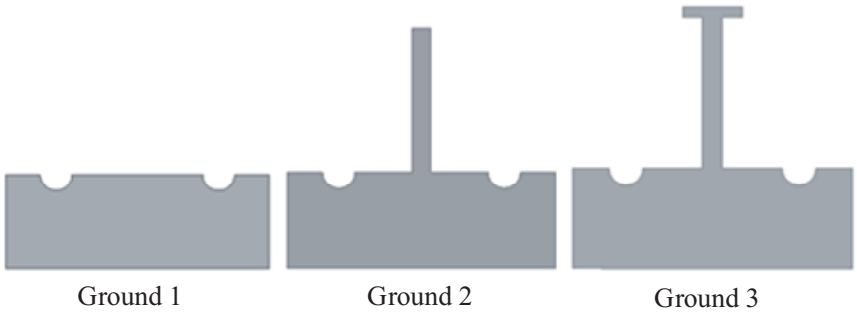

Figure 5. Configurations of the prototypes of Ground 1 to Ground 3.

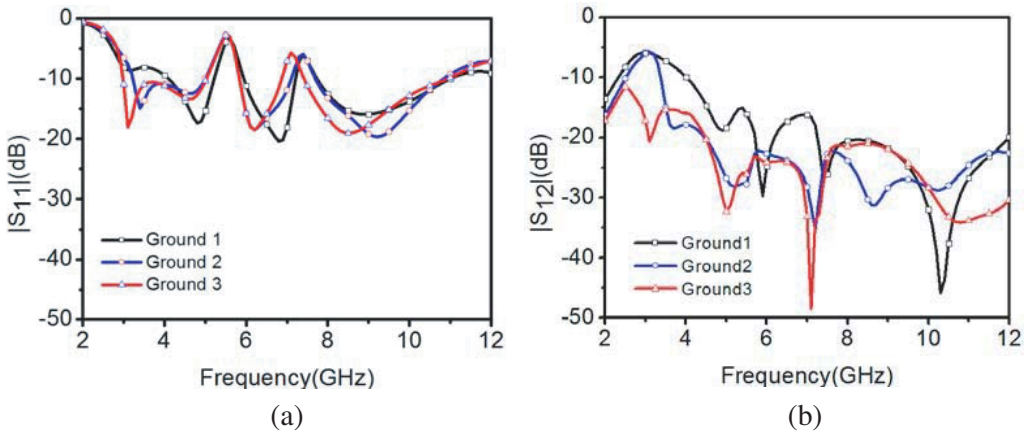

Figure 6. Simulated S-parameters of different ground planes. (a) $|S_{11}|$. (b) $|S_{12}|$.

antenna. The simulated S-parameters including S_{11} and S_{12} are illustrated in Figure 6. It can be seen from Figure 6 that the effect of the ground structure on the isolation is greater than reflections parameters. The S_{11} of Ground 1 has the highest cutoff frequency at about 4.3 GHz, and the isolation is very poor especially at low frequency. With the addition of the rectangle stub in Ground 2, the reflection parameter becomes better, but still does not meet the UWB requirements, and the isolation is poor in the frequency band below 3.4 GHz. In order to improve the impedance bandwidth and isolation at low frequency, a T-shaped (Ground 3) decoupling structure is introduced on the ground plane. The simulated results in Figures 6(a) and (b) show that the -10 dB impedance bandwidth and 15 dB isolation is achieved from 2.9 to 10.8 GHz, which meets the requirements of the UWB MIMO system.

3. RESULTS AND DISCUSSION

3.1. Scattering Parameters

The S-parameters of the proposed antenna is measured by an Agilent AV3672B vector network analyzer. Figure 7 shows the measured reflection and transmission characteristics. There is acceptable deviation between measured and simulated results due to fabrication tolerance. As depicted in Figure 7(a), the proposed antenna has an impedance bandwidth ($|S_{11}| \leq -10$ dB) from 2.9 GHz to 10.8 GHz except for

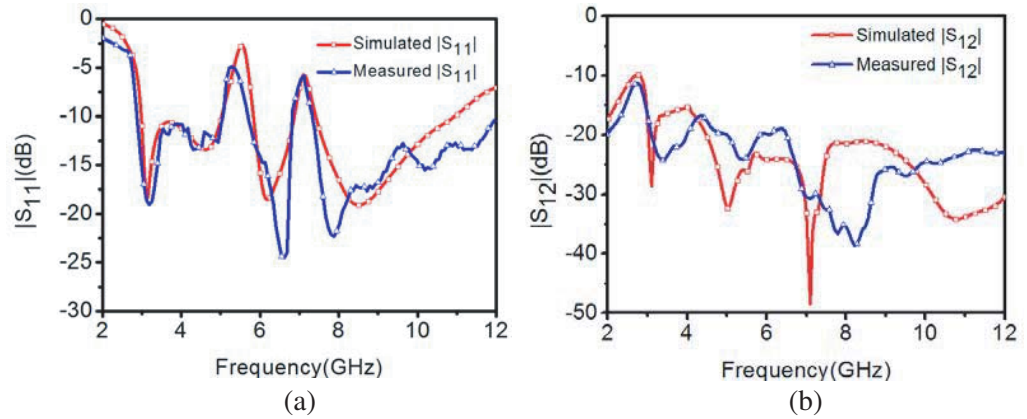

Figure 7. Simulated and measured S-parameters versus frequency of the proposed antenna. (a) $|S_{11}|$. (b) $|S_{12}|$.

5.15–5.85 GHz (WLAN band) and 6.7–7.1 GHz (IEEE INSAT/Super-Extended C-band). It can be seen from Figure 7(b) that the isolation ($|S_{12}|$) between two antenna elements is more than 15 dB through the whole working band.

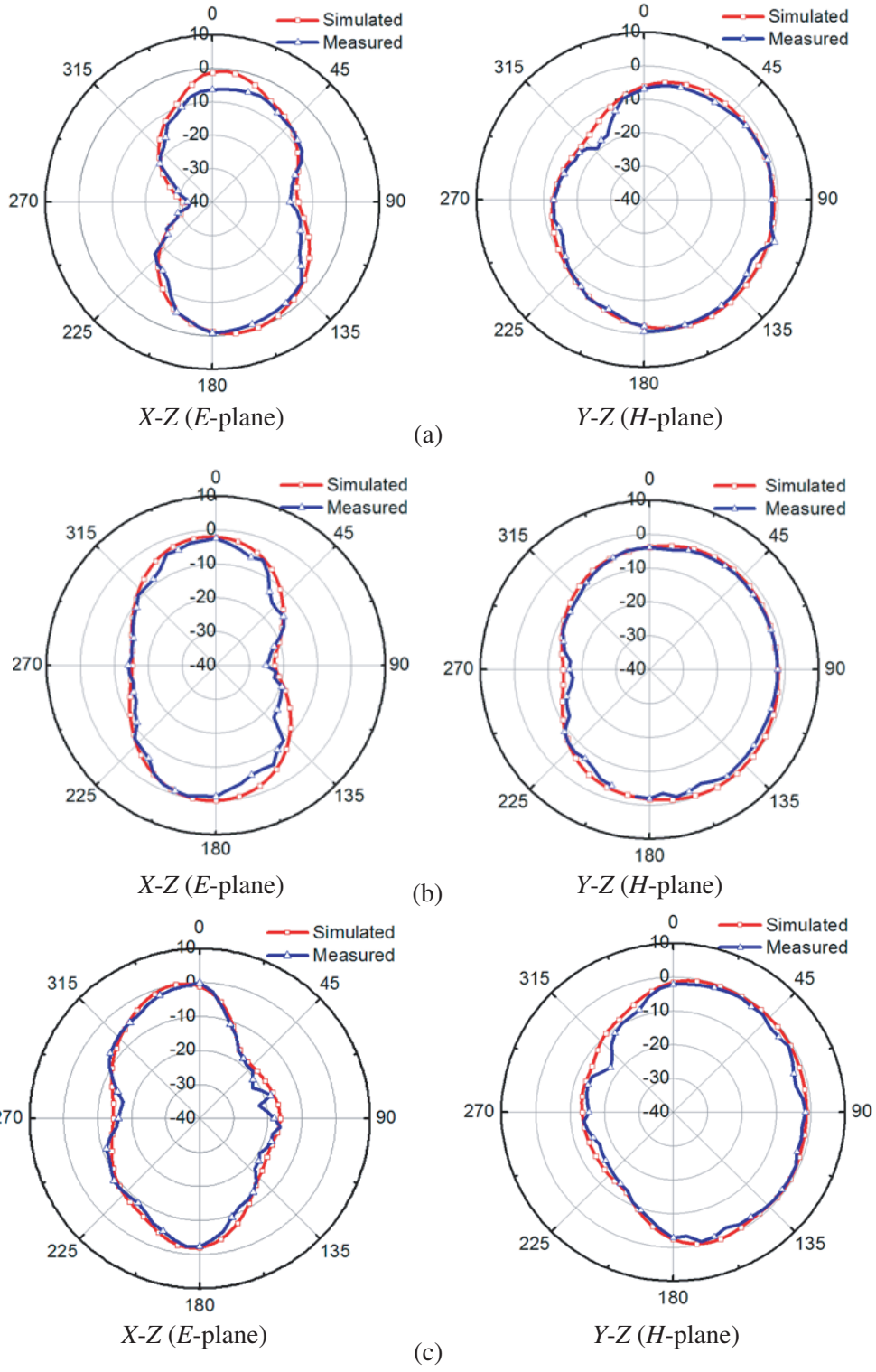

Figure 8. Simulated and measured radiation patterns of the proposed antenna. (a) 3 GHz. (b) 6.5 GHz. (c) 10 GHz.

3.2. Radiation Performance

The simulated and measured radiation patterns of the fabricated prototype are plotted in Figure 8 at frequencies of 3 GHz, 6.5 GHz, and 10 GHz, respectively, which include the X-Z plane (E plane) and Y-Z plane (H plane). Due to the symmetric antenna structure, the radiation patterns are measured in an anechoic chamber when port 1 is excited and port 2 terminated by a 50 Ω load. The measured results are in agreement with simulations.

3.3. Diversity Performance

Envelope correlation coefficient (ECC) is an important parameter whose value indicates the diversity performance of the MIMO antenna. In practical applications, ECC values below 0.5 denote perfect diversity performance. For a two-port antenna, ECC is calculated using [16]

$$\mathrm{ECC} = \frac{\left|S_{11}^{*}S_{12} + S_{21}^{*}S_{22}\right|^{2}}{\left(1 - \left(\left|S_{11}\right|^{2} + \left|S_{21}\right|^{2}\right)\right)\left(1 - \left(\left|S_{22}\right|^{2} + \left|S_{12}\right|^{2}\right)\right)}. \tag{3}$$

Figure 9 shows the ECC curves of the proposed antenna. It is observed that the ECC values are below 0.1 through the whole working band from 2.9 GHz to 10.8 GHz. The DG of the proposed UWB MIMO antenna can be calculated using

$$\mathrm{DG} = 10\sqrt{1 - \mathrm{ECC}^{2}} \tag{4}$$

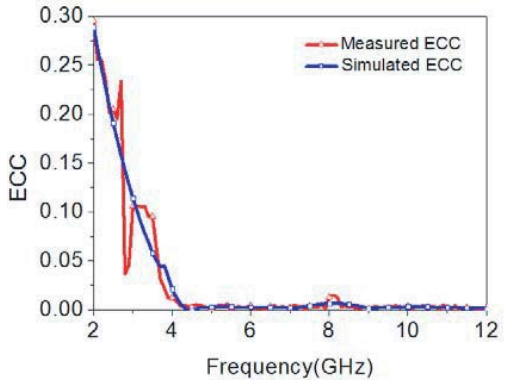

Figure 9. Simulated and measured ECC values versus frequency of the proposed antenna.

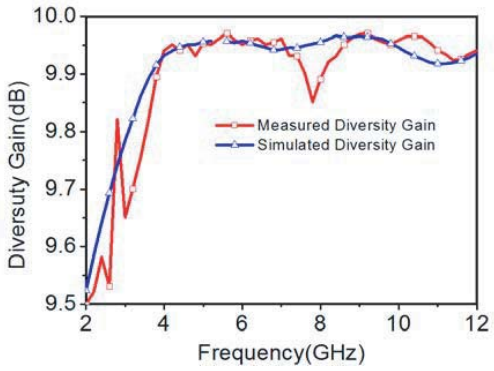

Figure 10. Simulated and measured DG values versus frequency of the proposed antenna.

It is observed that DG using S-parameters is ≥ 9.5 dB, as shown in Figure 10, which indicates that the proposed antenna has excellent diversity characteristics.

Figure 11 shows the multiplexing efficiency and peak gain with varying frequencies. Multiplexing efficiency (ηMUX) can be calculated by [17]

$$\eta\mathrm{MUX} = \sqrt{\left(1 - \left|\rho_c\right|^{2}\right)\eta_1\eta_2} \tag{5}$$

where ρ_c is the complex correlation coefficient between the two elements and ECC $\approx |\rho_c|^2$, η_i is the total efficiency of ith antenna element. From Figure 11 it is observed that at 5.5 GHz and 6.9 GHz ηMUX has a substantial drop. In addition, from Figure 11, peak gain drops to -14 dB at 5.5 GHz and -7.5 dB at 6.9 GHz, which means that the proposed antenna can perfectly avoid electromagnetic interference at notched band.

For multi-port antenna systems, adjacent antenna elements affect each other while operating simultaneously. It affects overall operational bandwidth and efficiency. Therefore, relying solely on S-parameters is not sufficient to predict actual system behavior. A new metric, expressed as total effective

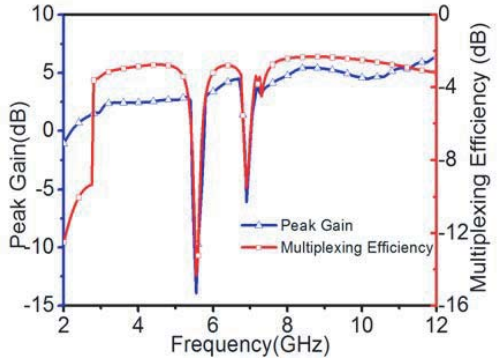

Figure 11. Multiplexing efficiency and Peak gain of the proposed antenna.

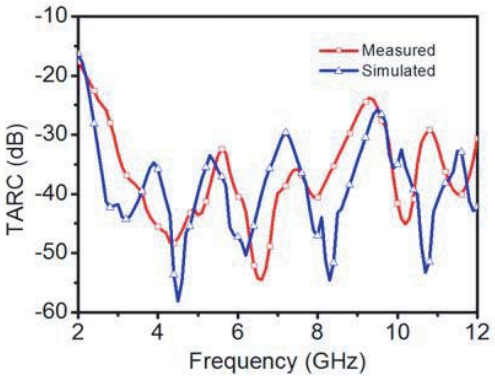

Figure 12. Simulated and measured TARC of the proposed antenna.

reflection coefficient (TARC), has been introduced to account for this effect. The TARC provides a more meaningful and complete MIMO efficiency characterization measurement because it contains the effect of mutual coupling. TARC can be defined as the square root of the ratio of total reflected power to total incident power and the apparent return loss of the entire MIMO antenna system. For dual-port MIMO system, it can be calculated by

$$\text{TARC} = \frac{\sqrt{(S_{11} + S_{12})^2 + (S_{21} + S_{22})^2}}{\sqrt{2}}. \tag{6}$$

For a MIMO communication system, the value of TRAC should < 0 dB. The measured and simulated values of TRAC are shown in Figure 12. It is observed from the figure that the value of TRAC for the proposed antenna is < -12 dB in the whole operating band.

4. CONCLUSION

A dual band-notched compact UWB MIMO antenna is investigated in this paper. The compact size of the antenna is 26 mm × 28 mm. The defected ground plane and tapered microstrip feeding lines are used to improve impedance matching, and the T-shaped stub on the ground is used to improve isolation. Simulated and measured results show that the proposed antenna has an impedance bandwidth from 2.9 to 10.8 GHz except for the WLAN and IEEE INSAT/Super-Extended C-band, and the isolation is more than 15 dB through the operating band. The ECC, DG, multiplexing efficiency, TARC and peak gain indicate that the diversity performance is excellent. All of the features mentioned above indicate that the proposed antenna is a good candidate for UWB diversity applications.

REFERENCES

1. Ma, T.-G. and S.-K. Jeng, "Planar miniature tapered-slot-fed annular slot antennas for ultrawideband radios," *IEEE Transactions on Antennas and Propagation*, Vol. 53, No. 3, 1194–1202, Mar. 2005.
2. Yang, Y., Q. Chu, and J. Li, "Dual band-notched ultrawideband MIMO antenna array," *2013 IEEE International Wireless Symposium (IWS)*, 1–4, Beijing, 2013.
3. Li, J., Q. Chu, and T. Huang, "A compact wideband MIMO antenna with two novel bent slits," *IEEE Transactions on Antennas and Propagation*, Vol. 60, No. 2, 482–489, Feb. 2012.
4. Ren, J., W. Hu, Y. Yin, and R. Fan, "Compact printed MIMO antenna for UWB applications," *IEEE Antennas and Wireless Propagation Letters*, Vol. 13, 1517–1520, 2014.
5. Zhu, J., S. Li, S. Liao, and Q. Xue, "Wideband low-profile highly isolated MIMO antenna with artificial magnetic conductor," *IEEE Antennas and Wireless Propagation Letters*, Vol. 17, No. 3, 458–462, Mar. 2018.

6. Toktas, A., M. Yerlikaya, K. Sabanci, A. Kayabasi, E. Yigit, and M. Tekbas, "Reducing mutual coupling for a square UWB MIMO antenna using various parasitic structures," *2017 10th International Conference on Electrical and Electronics Engineering (ELECO)*, 982–986, Bursa, 2017.
7. Iqbal, A., O. A. Saraereh, A. Bouazizi, and A. Basir, "Metamaterial based highly isolated MIMO antenna for portable wireless communication," *Electronics*, Vol. 7, No. 10, 2018.
8. Sokhi, I. K., R. Ramesh, and K. Usha Kiran, "Design of UWB-MIMO antenna for wireless applications," *2016 International Conference on Wireless Communications, Signal Processing and Networking (WiSPNET)*, 962–966, Chennai, 2016.
9. Joo, E., K. Kwon, J. Park, and J. Choi, "On-body UWB MIMO antenna for UWB application," *2013 Asia-Pacific Microwave Conference Proceedings (APMC)*, 1130–1132, Seoul, 2013.
10. Zhang, L., W. Liu, and T. Jiang, "A compact UWB MIMO antenna with high isolation," *2016 IEEE International Symposium on Antennas and Propagation (APSURSI)*, 913–914, Fajardo, 2016.
11. Liu, Y. and Z. Tu, "Compact differential band-notched stepped-slot UWB-MIMO antenna with common-mode suppression," *IEEE Antennas and Wireless Propagation Letters*, Vol. 16, 593–596, 2017.
12. Kang, L., H. Li, X. Wang, and X. Shi, "Compact offset microstrip-fed MIMO antenna for band-notched UWB applications," *IEEE Antennas and Wireless Propagation Letters*, Vol. 14, 1754–1757, 2015.
13. Gao, P., S. He, X. Wei, Z. Xu, N. Wang, and Y. Zheng, "Compact printed UWB diversity slot Antenna with 5.5-GHz band-notched characteristics," *IEEE Antennas and Wireless Propagation Letters*, Vol. 13, 376–379, 2014.
14. Zhu, J., et al., "A dual notched band MIMO slot antenna system with Y-shaped defected ground structure for UWB applications," *Microwave and Optical Technology Letters*, Vol. 58, No. 3, 626–630, 2016.
15. Taheri, M. M. S., H. R. Hassani, and S. M. A. Nezhad, "UWB printed slot antenna with bluetooth and dual notch bands," *IEEE Antennas and Wireless Propagation Letters*, Vol. 10, 255–258, 2011.
16. Blanch, S., J. Romeu, and I. Corbella, "Exact representation of antenna system diversity performance from input parameter description," *Electronics Letters*, Vol. 39, No. 9, 705–707, May 1, 2003.
17. Iqbal, A., O. A. Saraereh, A. W. Ahmad, and S. Bashir, "Mutual coupling reduction using F-shaped stubs in UWB-MIMO antenna," *IEEE Access*, Vol. 6, 2755–2759, 2018.